Sohag Journal of Mathematics
An International Journal

http://dx.doi.org/10.18576/sjm/080102

Peristaltic Motion of Micropolar Fluid With Slip Velocity in A Tapered Asymmetric Channel in Presence of Inclined Magnetic Field and Thermal Radiation

Ajaz Ahmad Dar

Department of Mathematics, Govt. Degree College, Chenani, Udhampur, Jammu and Kashmir, India.

Received: 23 Jun. 2020, Revised: 10 Dec. 2020, Accepted: 20 Dec. 2020
Published online: 1 Jan. 2021

Abstract: A study of an incompressible peristaltic flow of MHD micropolar fluid in a tapered irregular channel in a porous medium has been performed. The influence of aligned magnetic field, velocity slip and radiation has been taken into description. Heat source term is devised in the energy equation which promotes either generation or absorption. Long wavelength and low Reynolds number approach has been duly taken care of in the present investigation to simplify the governing equations of motion. The salient features of velocity, temperature, concentration and trapping are described with special emphasis on slip parameter, inclined magnetic number, thermal radiation, heat generation and non uniform parameter. Favorable comparison with previously available literature on various special issues of the problem has been prepared.

Keywords: MHD Micropolar fluid, Aligned Magnetic field, Tapered channel, Heat generation, Slip velocity, Thermal Radiation

1 Introduction

Importance of peristaltic motion of fluid is quite common in consideration of its physiological and engineering applications. Peristaltic motion plays an important role in allowing the food to muddle and shove ahead in the body parts due to area constriction and distension of channel walls. Peristalsis is an inherent property of many biological systems containing tubes of smooth muscles, transporting physiological liquids by its progressive movements. These kinds of flows expansively appear in the transport of chyme in the stomach, urine transport from kidney to bladder, movement of ovum in the fallopian duct, bile movement from gallbladder into the duodenum, circulation of blood in small capillaries, ingestion of food through esophagus, fluids in lymphatic vessels. Also its significance in chemical processes and medicinal diligence cannot be ignored as it covers novel pharmacological delivery systems, heart lung machine, blood pump in heart-lung machine, sanitized fluid transport, transport of mordant fluids, a poisonous liquid transportation in the nuclear production etc. Further the peristalsis in incidence of magnetic effects is vital in magneto-therapy, hyper-thermia, cancer therapy, atherosclerosis etc. The constrained application of low concentration and promptness pulsating fields revise the cell and tissue. Magnetic vulnerable of chyme is also fulfilled from the heat spawned by magnetic field or the ions enclosed in the chyme. The magnets might heat inflammations, ulceration and several infections of bowel (intestine) and uterus. Moreover, biomechanical engineer has confirmed now that rheological property is indispensable in the manufacturing and physiological dealings. Following the hypothetical and investigatory study initiated by Latham [1] and Shapiro et al. [2] the idea of peristalsis has been pursued by several other researchers. A quantity of recent explorations depicting the peristalsis of Newtonian and non-Newtonian fluids possibly have been examined in [3,4,5,6,7,8,9,10,28,29].

The modern industrial processes are exemplified by utilizing latest equipments which cannot be illustrated by Newtonian fluids. Due to this cause, various non-Newtonian models have been suggested. Eringen [11] first put forward the assumption of micropolar fluids to depict smooth media such as liquid crystals, ferro liquids, colloidal solutions, lubricants, liquid polymer stabilizers, clouds with smoke, fluid in brain, exotic

* Corresponding author e-mail: aijaz855141@gmail.com

emollients, low concentration suspensions, slurries and liquid crystals, animal blood carrying deformable particles (platelets), paints and turbulent shear flows etc. Actually, micropolar fluids incorporate a superior family of a lot more intricate Non-Newtonian fluids, that is, micromorphic liquids which include deformable micro-structured fluid elements, divulging innate motion individuality and having an irregular stress tensor. Expansive information of the constitutive equations of micropolar fluids are acknowledged in Lukaszewicz [12]. Micropolar fluids can prolong rotary motion with individual motions which shore up the stress and body moments and are manipulated by spin-inertia (Anwar et al.[13]). Micropolar fluids incorporate, as a special case, the well founded Navier-Stokes model of classical fluids that we shall entitle as ordinary fluids. Therefore, micropolar fluid provides a considerably more agreeable model for calculation than micromorphic fluids. Physically, such fluids may represent fluids containing rigid, haphazardly adjusted elements hovering in a gooey medium, where the perversion of fluid particles is disregarded. The associated numerical model is based on the introduction of a new vector field (the micro-rotation) which explains the overall angular velocity field of the particles rotation. Hence, we get an additional equation which represents the balance law of local angular momentum. Ashmawy [14] observed the influence of slip boundary conditions in fully developed natural convective micropolar fluid flow in a vertical channel. Ajaz and Elangovan [15] studied the problem of blood flow with a mild stenosis through a flat non-symmetric artery. Inspection of natural convection of micropolar fluid in a square cavity with uniform and non-uniform heated thin plate has been carried forward by Muthtamilselvan et al. [16]. Peristaltic transport of an incompressible non-Newtonian fluid in a non uniform channel has been pondered under the assumptions of long-wavelength and low-Reynolds number by Kothandapani et al.[17].

Radiation effects on MHD flow and convective heat transfer problems have become more essential industrially. Radiation effect can be reasonably critical at high operating temperatures. Scores of process in recent engineering areas crop up at high temperatures and comprehension of heat transfer with radiation turns out to be very significant for devising the relevant stuff, geothermal extractions, electrical power generation, impulsion devices for airplane, missiles, satellites, space vehicle re-entry, solar power technology, astrophysical flows and other engineering fields. An assortment of numerical models has been inspected in the past work in which effects of thermal radiation have been taken into consideration. The addition of heat dissemination term in temperature distribution equation ends in calculation intricacies for finding the solution of the partial-differential-equation. Though, several key estimations, such as, radiative conduction approximation might be used to scrutinize the elucidation of governing equations with radiative heat emission term. Ramzan et al.[18] studied the flow of a micropolar fluid with partial slip and convective boundary condition. Effects of transfer of heat and mass on unsteady magnetohydrodynamic flow of a viscoelastic micro-polar fluid under the influence of Hall effect and thermal radiation have been studied by Olajuwon et al.[19]. Ajaz and Elangovan [20] studied thermal radiation and inclined magnetic field effects on oscillatory flow in an irregular channel. Recently, Saddiqa et al.[21] analyzed the study of cyclic MHD ordinary convection boundary-layer flow of a radiating micro-polar fluid in close proximity to a perpendicular surface. Reddy et al. [30] studied thermal radiation effects on MHD Peristaltic Motion of Walters-B Fluid with Heat Source and Slip Conditions. Investigation of double diffusive heat and mass transfer characteristics of a micropolar fluid in existence of radiation has been carried out by Pal and Biswas [22]. Thermal analysis of MHD electro-osmotic peristaltic pumping of Casson fluid through a rotating asymmetric microchannel has been analyzed by Makinde et al. [31].

In recent times, physiologists analyzed that the intra-uterine fluid flow in a non-pregnant uterus because of myometrial contractions is peristaltic type motion and may occur in both symmetric and asymmetric directions. Additionally, it has been observed by Eytan and Elad [23] that intra-uterine fluid motion in a sagittal cross-section of the uterus stimulated by wall influenced peristaltic fluid flow in a two-dimensional channel with wave sprains containing a phase variation, moving autonomously on the both the walls. Also, Eytan et al. [24] examined that the width of the sagittal cross-section of the uterine crater enlarges in the direction of the fundus and the void is not entirely obstructed during the contractions. Further, it is meaningful to point out at this point that the intra-uterine fluid flow in a Sagittal section of the uterus releases a contracted channel enclosed by two somewhat parallel walls with wave sprains encompassing dissimilar amplitudes and phase dissimilarities [25,3]. Ellahi et al. [26] investigated heat and mass transfer in tapered stenosed arteries on micropolar fluid of blood flow with permeable walls. Ajaz Ahmad Dar [32] investigated the effect of Thermal radiation, temperature jump and inclined magnetic field on the peristaltic transport of blood flow in an asymmetric channel with variable viscosity and heat absorption/generation. Motivated by the investigations and consequences mentioned above, the intend of this article is to judge the influence of thermal emission and slip on micro-polar fluid through more generalized type of the channel, namely, the tapering asymmetric channel. In the current problem, slip velocity with aligned magnetic field influences are premeditated with high eminence. The extremely non-linear equations are rearranged by implementing low Reynolds number and long wavelength estimate and the phenomenon of trapping is also discussed.

2 Formulation of the problem

Mathematical model of micro-polar fluid in a tapering permeable channel of homogeneous thickness with aligned magnetic number is to be put up to discover the result of a choice of fluid parameters on biological constraints. Modeling is to be made by taking into account an uneven, standardized and electrically conducting micropolar fluid. The mathematical geometry of the problem is revealed in figure (1) and is articulated precisely as

$$Y' = H_2(X',t') = d + m'X' + a_2 \sin\left[\frac{2\pi}{\lambda}(X' - ct')\right]. \quad (1)$$

$$Y' = H_1(X',t') = -d - m'X' - a_1 \sin\left[\frac{2\pi}{\lambda}(X' - ct') + \Phi\right]. \quad (2)$$

Where X' is the direction of wave propagation and Y' is

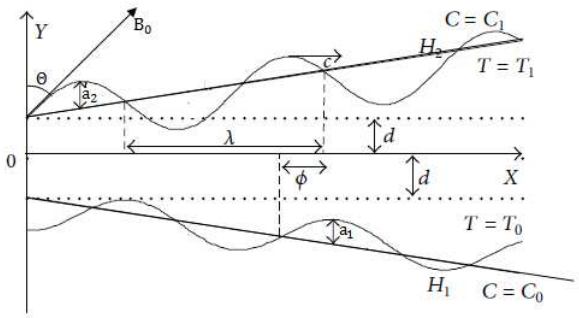

Fig. 1: The flow geometry

at right angles to it. The phase difference Φ fluctuates in the range $0 \le \Phi \le \pi$ in which $\Phi = 0$ corresponds to symmetric channel with waves out of phase and for $\Phi = \pi$, the waves are in phase. A uniform magnetic field is applied at an angle of Θ to the flow. The electric field is taken zero and the magnetic Reynolds number is taken small so that the induced magnetic field is negligible in comparison with the applied magnetic field. Further, a_1, b_1, d_1, d_2 and Φ satisfy the following condition

$$a_1^2 + b_1^2 + 2a_1 b_1 \cos\Phi \le (d_1 + d_2)^2. \quad (3)$$

The governing equations for unsteady flow of a micro-polar in the absence of viscous dissipation and body couples are given by

$$\frac{\partial u'}{\partial x'} + \frac{\partial v'}{\partial y'} = 0. \quad (4)$$

$$\rho\left(\frac{\partial u'}{\partial t'} + u'\frac{\partial u'}{\partial x'} + v'\frac{\partial u'}{\partial y'}\right) = -\frac{\partial p'}{\partial x'} - \frac{\mu}{K_1'}(u'+1) + (\mu + k)\left(\frac{\partial^2 u'}{\partial x'^2} + \frac{\partial^2 u'}{\partial y'^2}\right) + k\frac{\partial g'}{\partial y'} - \sigma B_0^2 \cos\Theta\left(\cos\Theta(u'+c) - v'\sin\Theta\right). \quad (5)$$

$$\rho\left(\frac{\partial v'}{\partial t'} + u'\frac{\partial v'}{\partial x'} + v'\frac{\partial v'}{\partial y'}\right) = -\frac{\partial p'}{\partial y'} - \frac{\mu}{K_1'}(v') + (k + \mu)\left(\frac{\partial^2 v'}{\partial x'^2} + \frac{\partial^2 v'}{\partial y'^2}\right) - k\frac{\partial g'}{\partial x'} + \sigma B_0^2 \sin\Theta\left\{\cos\Theta(u'+c) - v'\sin\Theta\right\}. \quad (6)$$

$$\rho j'\left(\frac{\partial g'}{\partial t'} + u'\frac{\partial g'}{\partial x'} + v'\frac{\partial g'}{\partial y'}\right) = -2kg' + \gamma\left(\frac{\partial^2 g'}{\partial x'^2} + \frac{\partial^2 g'}{\partial y'^2}\right) + k\left(\frac{\partial v'}{\partial x'} - \frac{\partial u'}{\partial y'}\right). \quad (7)$$

$$\rho c_p\left(\frac{\partial T'}{\partial t'} + u'\frac{\partial T'}{\partial x'} + v'\frac{\partial T'}{\partial y'}\right) = K'\left(\frac{\partial^2 T'}{\partial x'^2} + \frac{\partial^2 T'}{\partial y'^2}\right) - \frac{\partial q_r}{\partial y'} + Q'(T' - T_0). \quad (8)$$

$$\left(\frac{\partial C'}{\partial t'} + u'\frac{\partial C'}{\partial x'} + v'\frac{\partial C'}{\partial y'}\right) = D_m\left(\frac{\partial^2 C'}{\partial x'^2} + \frac{\partial^2 C'}{\partial y'^2}\right) + \frac{D_m K_T}{T_m}\left(\frac{\partial^2 T'}{\partial x'^2} + \frac{\partial^2 T'}{\partial y'^2}\right). \quad (9)$$

where u' and v' are the velocity components in the x' and y' directions, respectively, C' is the concentration, T' is temperature.

We employ the subsequent non-dimensional variables in the above governing equations

$$x = \frac{x'}{\lambda}, y = \frac{y'}{d}, \delta = \frac{d}{\lambda}, K = \frac{K_1'}{d^2}, v = \frac{v'}{\delta c}, t = \frac{ct'}{\lambda}$$
$$p = \frac{p'd^2}{c\lambda\mu}, j = \frac{j'}{d^2}, g = \frac{dg'}{c}, M = \sqrt{\frac{\sigma}{\mu}}dB_0, R_e = \frac{\rho cd}{\mu}$$
$$h_2 = \frac{H_2}{d}, u = \frac{u'}{c}, \theta = \frac{T' - T_0}{T_1 - T_0}, \phi = \frac{C' - C_0}{C_1 - C_0}, P_r = \frac{\mu c_p}{K'}$$
$$S_r = \frac{\rho D_m K_T (T_1 - T_0)}{T_m \mu (C_1 - C_0)}, a = \frac{a_1}{d}, m_1 = \frac{m'\lambda}{d}, b = \frac{b_1}{d}$$
$$S_c = \frac{\mu}{\rho D_m}, h_1 = \frac{H_1}{d}, Q = \frac{Q'd^2}{c_p\mu}, N_r = \frac{16\sigma' T_0^3}{3k'K'}. \quad (10)$$

The radiative flux q_r for radiation is obtained by applying Rosseland diffusion approximation, and is given as

$$q_r = -\frac{4\sigma'}{3k'}\frac{\partial T'^4}{\partial y'}. \quad (11)$$

It is well-known that the substantial radiation limit is considered in this study. Assuming that the temperature inconsistencies inside the course of flow are passably minute, hence, T'^4 can be embodied as the linear function of temperature and is adapted by applying Taylor expansion on T'^4 about T_0 as mentioned below

$$T'^4 = T_0^4 + 4T_0^3(T'-T_0) + 6T_0^2(T'-T_0)^2 + ----. \tag{12}$$

By neglecting the higher powers of T (higher than first) in $(T'-T_0)$, we get

$$T'^4 \approx -3T_0^4 + 4T_0^3 T'. \tag{13}$$

From Equation.(11) and (13), we obtain

$$\frac{\partial q_r}{\partial y'} = -\frac{16\sigma' T_0^3}{3k'}\frac{\partial^2 T'}{\partial y'^2}. \tag{14}$$

The modified governing equations in terms of non-dimensional quantities are as follows

$$R_e\delta\left(u\frac{\partial u}{\partial x}+v\frac{\partial u}{\partial y}\right) = -\frac{\partial p}{\partial x}+\frac{(\mu+k)}{\mu}\left(\delta^2\frac{\partial^2 u}{\partial x^2}+\frac{\partial^2 u}{\partial y^2}\right) + \frac{k}{\mu}\frac{\partial g}{\partial y} - M^2\cos\Theta\left((u+1)\cos\Theta - v\delta\sin\Theta\right) - \frac{u+1}{K}. \tag{15}$$

$$R_e\delta^3\left(u\frac{\partial v}{\partial x}+v\frac{\partial v}{\partial y}\right) = -\frac{\partial p}{\partial y}+\frac{(\mu+k)}{\mu}\delta^2\left(\delta^2\frac{\partial^2 u}{\partial x^2}+\frac{\partial^2 u}{\partial y^2}\right) - \delta^2\frac{k}{\mu}\frac{\partial g}{\partial x} + M^2\delta\sin\Theta\left((u+1)\cos\Theta - v\delta\sin\Theta\right) - \delta^2\frac{v}{K}. \tag{16}$$

$$\rho a c j\delta\left(u\frac{\partial g}{\partial x}+v\frac{\partial g}{\partial y}\right) = -2kg + \frac{\gamma}{a^2}\left(\delta^2\frac{\partial^2 g}{\partial x^2}+\frac{\partial^2 g}{\partial y^2}\right) + k\left(\delta^2\frac{\partial v}{\partial x}-\frac{\partial u}{\partial y}\right). \tag{17}$$

$$R_e\delta\left(u\frac{\partial \theta}{\partial x}+v\frac{\partial \theta}{\partial y}\right) = \frac{1}{P_r}\left(\delta^2\frac{\partial^2\theta}{\partial x^2}+\frac{\partial^2\theta}{\partial y^2}\right) + \frac{N_r}{P_r}\frac{\partial^2\theta}{\partial y^2} + Q\theta. \tag{18}$$

$$R_e\delta\left(u\frac{\partial \phi}{\partial x}+v\frac{\partial \phi}{\partial y}\right) = \frac{1}{S_c}\left(\delta^2\frac{\partial^2\phi}{\partial x^2}+\frac{\partial^2\phi}{\partial y^2}\right) + S_r\left(\delta^2\frac{\partial^2\theta}{\partial x^2}+\frac{\partial^2\theta}{\partial y^2}\right). \tag{19}$$

Using low Reynolds number and long wavelength approximation, the equations (15)-(19) can be written as

$$(1-N)\frac{\partial p}{\partial x} = \frac{\partial^2 u}{\partial y^2}+N\frac{\partial g}{\partial y} - (1-N)\left(\frac{1}{K}+M^2\cos^2\Theta\right)(u+1). \tag{20}$$

$$\frac{\partial p}{\partial y} = 0. \tag{21}$$

$$2g = -\frac{\partial u}{\partial y}+\left(\frac{2-N}{m^2}\right)\frac{\partial^2 g}{\partial y^2}. \tag{22}$$

$$(1+N_r)\frac{\partial^2\theta}{\partial y^2}+P_r Q\theta = 0. \tag{23}$$

$$\frac{\partial^2\phi}{\partial y^2}+S_c S_r\frac{\partial^2\theta}{\partial y^2} = 0. \tag{24}$$

here $N = \frac{k}{(k+\mu)}$ is the coupling number in the range $(0 \le N \le 1)$ and $m^2 = \frac{a^2 k(2\mu+k)}{\gamma(\mu+k)}$ is the micropolar fluid parameter.

The boundary conditions in terms of dimensionless quantities are given as

$$u = -1-\beta\frac{\partial u}{\partial y}, \quad \theta = 0, \quad \phi = 0 \quad at \quad y = h_1 = -1-m_1 x - a\sin[2\pi(x-t)+\Phi]. \tag{25}$$

$$u = -1+\beta\frac{\partial u}{\partial y}, \quad \theta = 1, \quad \phi = 1 \quad at \quad y = h_2 = 1+m_1 x + b\sin[2\pi(x-t)+]. \tag{26}$$

$$g = 0 \qquad at \qquad y = h_1 \text{ and } h_2. \tag{27}$$

β is the dimensionless slip parameter.

3 Method of Solution

Equation.(21) depicts that p is not a function of y. Hence, $\frac{\partial p}{\partial x} = \frac{dp}{dx}$.
Differentiate Equation.(21) with respect to y to get

$$\frac{\partial^2 u}{\partial y^2} = -2\frac{\partial g}{\partial y}+\left(\frac{2-N}{m^2}\right)\frac{\partial^3 g}{\partial y^3}. \tag{28}$$

Using Equation.(28) in Equation.(20), one obtains

$$u = \frac{1}{(1-N)\left(M^2\cos^2\Theta+\frac{1}{K}\right)}\left\{\left(\frac{2-N}{m^2}\right)\frac{\partial^3 g}{\partial y^3} - (2-N)\frac{\partial g}{\partial y}\right\} - \frac{1}{(1-N)\left(M^2\cos^2\Theta+\frac{1}{K}\right)}\left\{(1-N)\frac{dp}{dx}\right\} \tag{29}$$

Using Equation.(29) in Equation.(22), we get

$$\frac{\partial^4 g}{\partial y^4} - \left\{(1-N)\left(M^2\cos^2\Theta+\frac{1}{K}\right)+m^2\right\}\frac{\partial^2 g}{\partial y^2} + \frac{2m^2\left\{(1-N)\left(M^2\cos^2\Theta+\frac{1}{K}\right)\right\}}{2-N}g = 0. \tag{30}$$

The general solution of Equation.(30) is given by

$$g = C_1 e^{A_1(-y)} + C_2 e^{A_1 y} + C_3 e^{A_2(-y)} + C_4 e^{A_2 y}. \tag{31}$$

where

$$A_1 = \frac{1}{\sqrt{2}}\sqrt{m_3 - \sqrt{m_3^2 - 4m_2}}$$
$$A_2 = \frac{1}{\sqrt{2}}\sqrt{m_3 + \sqrt{m_3^2 - 4m_2}}. \tag{32}$$

$$m_2 = \frac{2m^2(1-N)\left(M^2\cos^2\Theta + \frac{1}{K}\right)}{2-N}$$
$$m_3 = (1-N)\left(M^2\cos^2\Theta + \frac{1}{K}\right) + m^2. \tag{33}$$

The expression of axial velocity can be obtained by substituting Equation.(31) in Equation.(29). After applying the boundary conditions from Eqs.(25-27), the axial velocity is given as

$$u = B_1\left(A_1C_2e^{A_1y} - A_1C_1e^{A_1(-y)}\right)$$
$$+B_2\left(A_2C_4e^{A_2y} - A_2C_3e^{A_2(-y)}\right) - B_6. \tag{34}$$

where

$$B_1 = \frac{A_1(2-N)\left(\frac{A_1^2}{m^2} - 1\right)}{m_3 - m^2},\ B_2 = \frac{A_2(2-N)\left(\frac{A_2^2}{m^2} - 1\right)}{m_3 - m^2}$$
$$B_3 = A_1^2\beta B_1\left(e^{A_1h_1} - e^{A_1h_2}\right)\left(e^{A_2h_1} - e^{A_2h_2}\right). \tag{35}$$

$$B_4 = A_2B_2\left(e^{A_1h_1} - e^{A_1h_2}\right)\left((1-A_2\beta)e^{A_2h_2} + (A_2\beta+1)e^{A_2h_1}\right). \tag{36}$$

$$B_5 = A_1B_1\left(e^{A_1h_1} + e^{A_1h_2}\right)\left(e^{A_2h_1} - e^{A_2h_2}\right) + B_3 - B_4$$
$$B_6 = \frac{1-K}{m_3 - m^2}\frac{dp}{dx}. \tag{37}$$

$$C_1 = \frac{(1-B_6)e^{A_1(h_1+h_2)}\left(e^{A_2h_1} - e^{A_2h_2}\right)}{B_5}$$
$$C_2 = \frac{(B_6-1)\left(e^{A_2h_1} - e^{A_2h_2}\right)}{B_5}. \tag{38}$$

$$C_3 = \frac{(B_6-1)e^{A_2(h_1+h_2)}\left(e^{A_1h_1} - e^{A_1h_2}\right)}{B_5}$$
$$C_4 = \frac{(1-B_6)\left(e^{A_1h_1} - e^{A_1h_2}\right)}{B_5}. \tag{39}$$

The expressions for the energy and concentration distributions can be attained upon resolving Equation.(23) and Equation.(24) using dimensionless boundary conditions. The mathematical expressions for temperature θ and concentration ϕ are specified as follows

$$\theta(y) = \frac{\sinh(A_3h_1)\cosh(A_3y) - \cosh(A_3h_1)\sinh(A_3y)}{\sinh(A_3h_1)\cosh(A_3h_2) - \sinh(A_3h_2)\cosh(A_3h_1)}. \tag{40}$$

$$\phi(y) = \frac{S_cS_r\left(\cosh(A_3h_1)\sinh(A_3y) - \sinh(A_3h_1)\cosh(A_3y)\right)}{\sinh(A_3h_1)\cosh(A_3h_2) - \sinh(A_3h_2)\cosh(A_3h_1)}$$
$$+\frac{(h_1-y)(S_cS_r+1)}{h_1-h_2}. \tag{41}$$

where

$$A_3 = \sqrt{\frac{QP_r}{1+N_r}}.$$

In the wave frame of reference, the flux q is given as

$$q = \int_{h_2}^{h_1} u(x,y)dy = B_1C_1\left(e^{-A_1h_1} - e^{-A_1h_2}\right)$$
$$+B_1C_2\left(e^{A_1h_1} - e^{A_1h_2}\right) + B_2C_3\left(e^{-A_2h_1} - e^{-A_2h_2}\right)$$
$$+B_2C_4\left(e^{A_2h_1} - e^{A_2h_2}\right) + B_6(h_2 - h_1). \tag{42}$$

Equation.(40) gives the pressure gradient equation and can be written as

$$\frac{dp}{dx} = -A_4B_1\left(C_1\left(e^{-A_1h_1} - e^{-A_1h_2}\right) + C_2\left(e^{A_1h_1} - e^{A_1h_2}\right)\right)$$
$$-A_4B_2\left(C_3\left(e^{-A_2h_1} - e^{-A_2h_2}\right) + C_4\left(e^{A_2h_1} - e^{A_2h_2}\right)\right) + A_4q. \tag{43}$$

The dimensionless expression for rise in pressure Δp over one wavelength is given as follows

$$\Delta p = \int_0^1 \left(\frac{dp}{dx}\right)dx. \tag{44}$$

Introducing the stream function $u = \frac{\partial\psi}{\partial y}$ and $v = -\delta\frac{\partial\psi}{\partial x}$, one can find that

$$\psi = B_1C_1e^{A_1(-y)} + B_1C_2e^{A_1y} + B_2C_3e^{A_2(-y)}$$
$$+B_2C_4e^{A_2y} - B_6y. \tag{45}$$

The dimensionless Skin Friction at $y = h_1$ and $y = h_2$ is given by

$$\tau_{h_1} = -\left(\frac{\partial u}{\partial y}\right)_{h_1} \qquad \tau_{h_2} = -\left(\frac{\partial u}{\partial y}\right)_{h_2} \tag{46}$$

The local Nusselt Number along the walls of the channel can be expressed as

$$N_u = \frac{dq_w}{K'(T_1 - T_0)},\ \text{where}\ \ q_w = -K'\frac{\partial T'}{\partial y'} \tag{47}$$

The dimensionless Nusselt Number at $y = h_1$ and $y = h_2$ is given by

$$N_{uh_1} = -\left(\frac{\partial \theta}{\partial y}\right)_{h_1} \qquad N_{uh_2} = -\left(\frac{\partial \theta}{\partial y}\right)_{h_2} \tag{48}$$

The Sherwood Number along the walls of the channel can be expressed as

$$Sh = \frac{dq_m}{D_m(C_1 - C_0)}, \text{ where } \quad q_m = -D_m \frac{\partial C'}{\partial y'} \tag{49}$$

The dimensionless Sherwood Number at $y = h_1$ and $y = h_2$ is given by

$$Sh_{h_1} = -\left(\frac{\partial \phi}{\partial y}\right)_{h_1} \qquad Sh_{h_2} = -\left(\frac{\partial \phi}{\partial y}\right)_{h_2} \tag{50}$$

4 Numerical results and discussion

The aim of this section is to depict the physical characteristics of a range of ensconced parameter in the acknowledged flow problems on the axial velocity, micro-rotation, temperature distribution, concentration distribution and stream function which are illustrated in Figs. 2?6. To analyze the conduct of axial velocity, mathematical computations for several values of micropolar material parameter m, slip parameter β, Hartmann number M, Eringen coupling parameter N, the non uniform parameter of the channel (m_1), inclination of magnetic field Θ, and the porous parameter K have been carried out in Fig.2. It is practical from Figs. 2(a), 2(c) and 2(d) that the axial velocity (u) diminishes by escalating magnetic field parameter, slip parameter and Eringen coupling parameter respectively. These outcomes are in good harmony with the results attained by Shit and Roy [27]. The enhance in the magnetic field parameter decreases the velocity because magnetic field gives rise to a resistive force called as the Lorentz Force. This force slows down the motion of the fluid. This result has a fundamental role in almost all industrial applications, mainly in support to solidification methods for instance, casting and semiconductor single crystal growth applications. In these states, as the liquids experience solidification, fluid flow and turbulence occur in the solidifying liquid pool and have critical conclusions on the product quality control. The practice of magnetic fields has efficiently been applied to monitoring melt convection in solidification systems. Also the utilization of magnetic particles in the healing of cancer is less focused on the delivery of drugs and more on their use as a new therapeutic outset in which tumor cells are blemished by applying local heat through an external magnetic field. Figs. 2(b), 2(e) and 2(f) illustrates that the axial velocity enhances by increasing the porous parameter, the aligned magnetic field parameter and the micropolar fluid parameter.

Fig.3 gives emphasis on the influence of various embedded parameters on micro-rotation (g). Fig.3(a) that the micro-rotation dwindles in the upper half of an asymmetric channel while in the lower half of the channel, it boosts up by enhancing M. It stipulates that the rotation about the middle of the channel takes place in two opposed ways in micro-particles. The increase in Hartmann number M makes the center of rotation to get transferred near the boundary of the channel. In comparison to Hartmann number effect on micro-rotation, an opposite trend is noticed by following parameters, namely, coupling number, aligned magnetic field, porous parameter, micropolar parameter and slip parameter as shown in Fig.3(b)-(f).

The effect of various embedded parameters over temperature profile is described in Fig.4. It portrays the impact of Prandtl number (P_r), thermal Radiation (N_r), Heat source parameter (Q) and non-uniform parameter (m_1) on temperature profile. Effect of thermal radiation on temperature is shown in Fig.4(a), which depicts decrease in temperature by increasing radiation parameter. While, Prandtl number and Heat source parameters show opposite nature to that of thermal radiation (See Figs. 4(b) and 4(c)). Changes in temperature by non-uniform parameter is observed in Fig. 4(d). It is illustrated that the temperature increases in the region $y \in [-1.5, 0.22]$ after that the situation is reversed with increasing m_1. Fig.5 illustrates the concentration distribution variation for different values of N_r, P_r, Q, m_1, S_c and S_r. It is noted that the embedded parameters show exactly opposite behavior on concentration distribution when compared with the temperature distribution. The concentration increases by increasing the thermal radiation parameter (N_r) and decreases by increasing Prandtl number (P_r) and Heat source parameter (Q). It is also illustrated from Fig.5(e)-(f) that the concentration distribution increases with an increase of Schmidt number (S_c) and Soret number (S_r).

Trapping is one more fascinating subject in peristaltic phenomenon. The pattern of an internally circulating bolus of fluid through closed streamlines is called trapping and this ensnared bolus is pressed forward down the peristaltic wave. Fig.6 presents the streamline hallucinations for the influence of Magnetic field M and non-uniform parameter (m_1). Significantly different patterns are observed. The effect of dissimilar values of magnetic number M on streamlines have been designed in figs. 6(a and b) keeping other parameters fixed. It is noticeable that the volume of the bolus reduces by enhancing M. The effect of non-uniform parameter m_1 on trapping is described in figs.6(c and d). It is inspected that the bolus size increases by increasing m_1. Fig.7 presents the streamline images for the effect of the coupling number N and amplitude ratio a. Fig 7(a) explains the deviation of streamlines by coupling number. It is monitored that the volume of the bolus shrinks with increasing N. The streamlines for various values of a are given away in Fig.7(b). It is noticed that the bolus size decreases with increasing a. These results hold good with

the results obtained by Kothandapani et al. [17].

Fig. 8 shows the effects of skin fiction with the Magnetic field (M) and porous parameter (K) at the top and bottom of the channel. In Fig. 8(a) and 8(b), it is found that skin fiction increases with the increase of the Magnetic field at the bottom of the channel whereas an opposite trend is observed at the top of the channel. It can be noted in Fig. 8(c) that at the bottom of the channel the skin fiction decreases with increasing the Porous parameter while at the top of the channel in Fig. 8(d), skin fiction increases with increasing the Porous parameter. Fig. 9 shows the effects of Nusselt number for different values of thermal radiation parameter (Nr) and Heat source parameter (Q). In Fig. (9a), it can be seen that Nusselt number decreases by increasing the values of thermal radiation parameter. While at the top of the channel, the Nusselt number increases with the increase of thermal radiation parameter. From Fig. (9c) and 9(d), it can be observed that the behavior of Heat source parameter on Nusselt number is totally opposite as compared to thermal radiation parameter. Fig.(10) illustrates the variation of Sherwood number for different parameters. In Fig. 10(a)-(bottom of the channel), it is observed that by increasing the thermal radiation parameter (N_r), the Sherwood number also increases. While at the top of the channel (Fig. 10(b)), an opposite behavior is observed. Fig. 10(c)-(bottom of the channel) shows the profile of the Sherwood number S_h along the wavy channel at various values of Prandtl number (P_r). Sherwood number decreases with increasing values of Prandtl number. In Fig. 10(d)-(top of the channel), it is noticed that when the Prandtl number P_r increases, the peak value of the Sherwood number S_h increases as well. The minimum values of the Sherwood number S_h occur slightly upstream of the maximum cross sections of the channel. In Fig. 10(e) and 10(f), it is noticed that the effect of Schmidt number (S_c)r on Sherwood number is similar as compared to the Prandlt number.

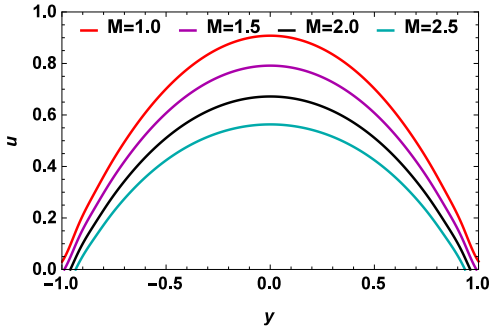

2a

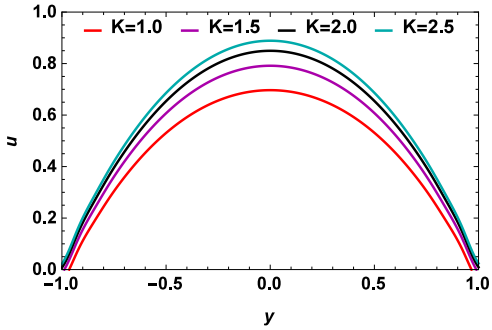

2b

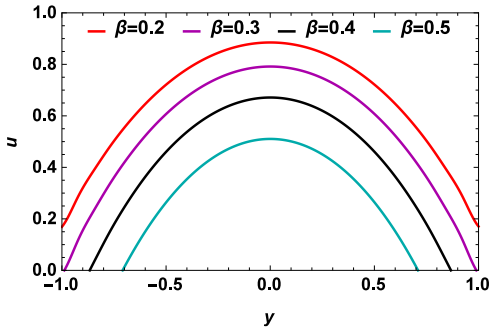

2c

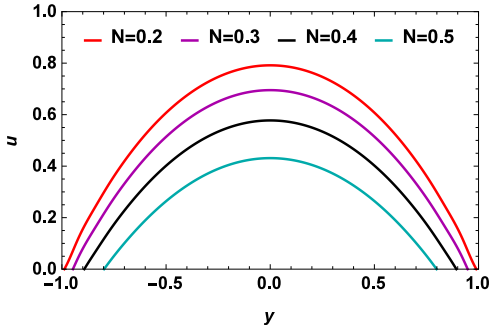

2d

5 Conclusion

In this study, an investigation on MHD micropolar fluid in the presence of a tapered asymmetric wavy channel has been carried out. The salient features trapping are presented with special focus on m_1, N and M. The nonlinear and coupled governing equations are decoded methodically by low Reynolds number and long wavelength approximations. Mathematical outcome are obtained to demonstrate the details of the flow, heat and mass transfer characteristics and their dependence on material parameters. The key conclusions are given as:

- –The axial velocity diminishes by increasing M, N and β, while a reverse trend is noticed by increasing porous parameter and micropolar fluid parameter.
- –The axial velocity increases by increasing the angle of inclination of the magnetic field. It indicates that the stream velocity enhances from flat to the vertical channel.
- –It is noticed that the micro-rotation enhances in the lower branch of the channel whereas it confirms a decrease in the upper half of the channel by increasing magnetic parameter. The other parameters of interest

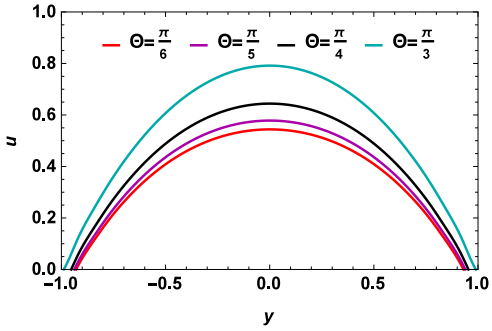

2e

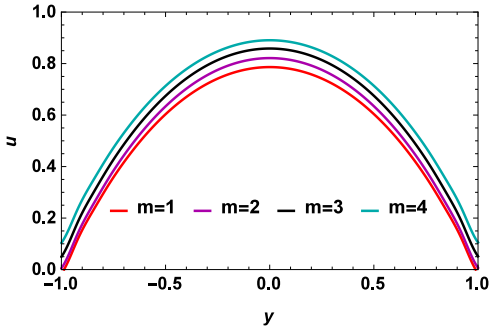

2f

Fig. 2: Effect of embedded parameters on the axial velocity u when $a = 0.1, b = 0.5, m_1 = 1.3, t = 0.5, x = 0.7, \frac{dp}{dx} = -2, \phi = \frac{\pi}{3}$

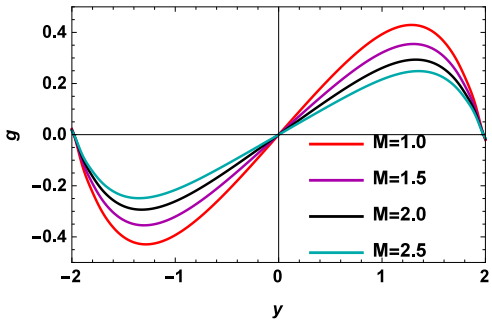

3a

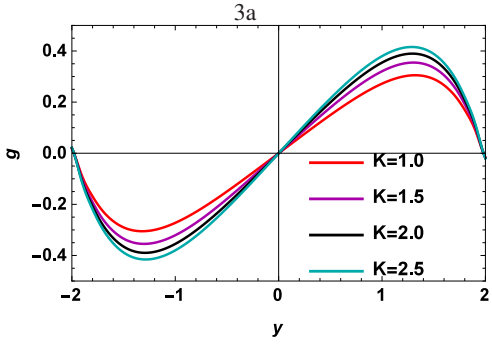

3b

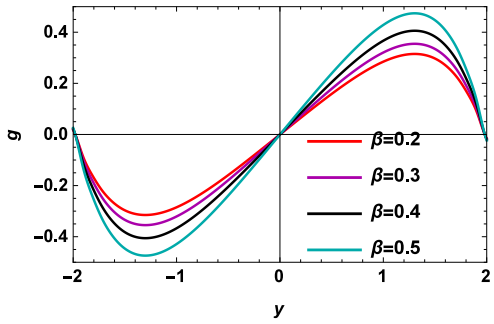

3c

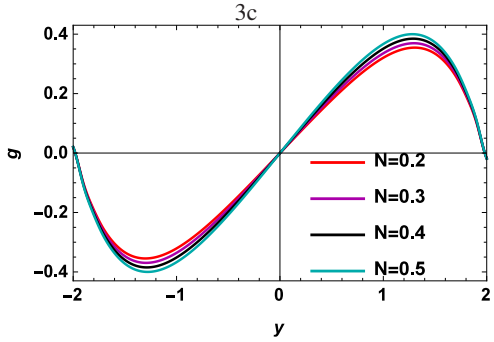

3d

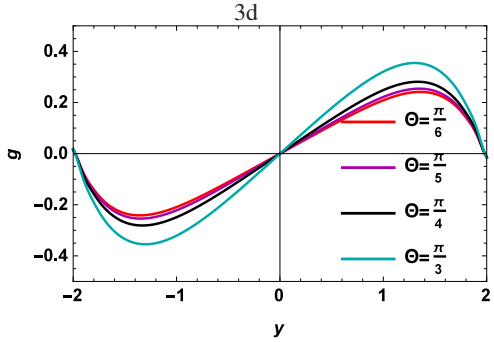

3e

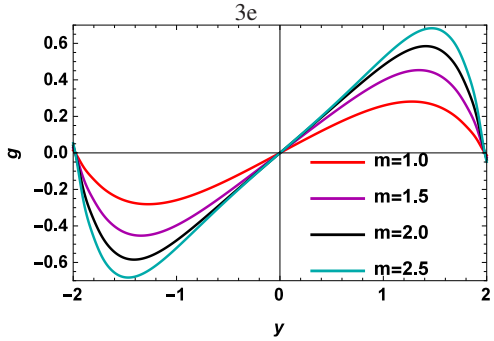

3f

Fig. 3: Variation in micro-rotation when $a = 0.1, b = 0.5, m_1 = 1.3, t = 0.5, x = 0.7, \frac{dp}{dx} = -2, \phi = \frac{\pi}{3}$

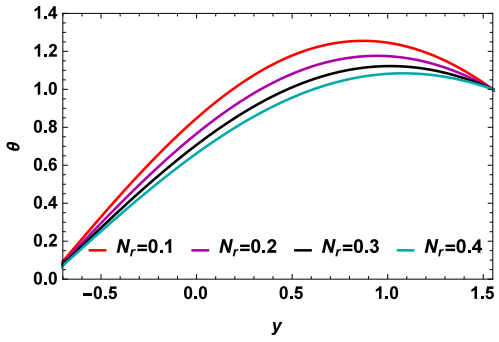

4a

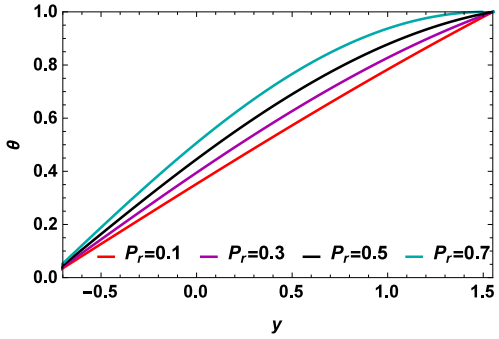

4b

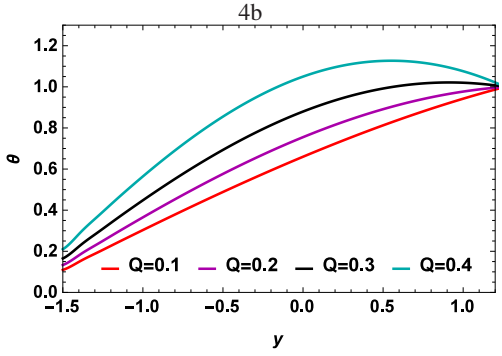

4c

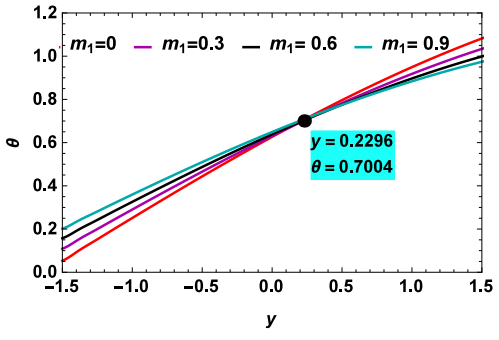

4d

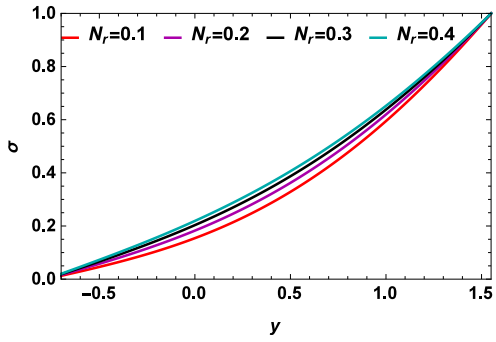

5a

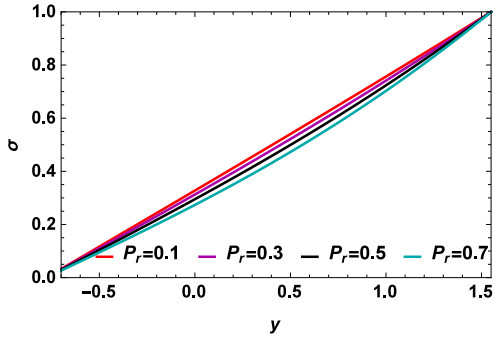

5b

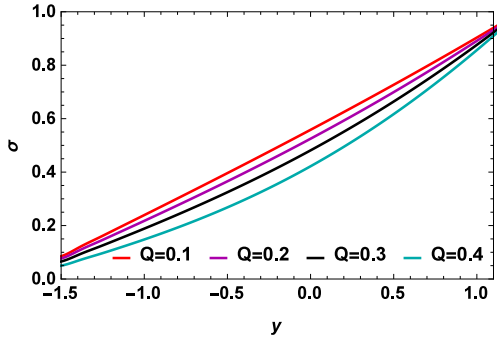

5c

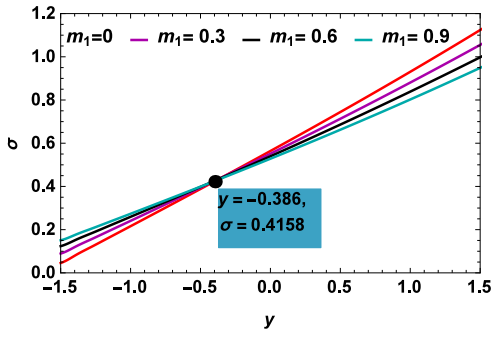

5d

Fig. 4: Variation in Temperature profile (θ) when $a = 0.4, b = 0.5, t = 0.2, x = 0.5, \phi = \frac{2\pi}{3}$

.

show opposite behavior on spin velocity in comparison with magnetic number.

–Increase in thermal radiation effect, decreases temperature distribution while it gets increased by heat source and Prandtl number.

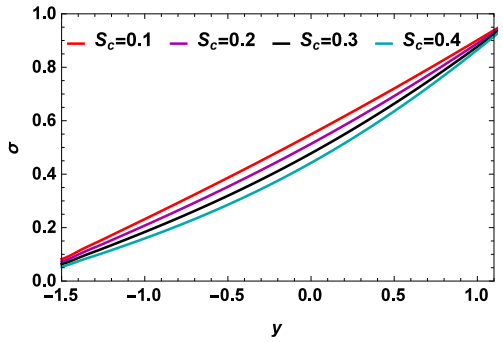

5e

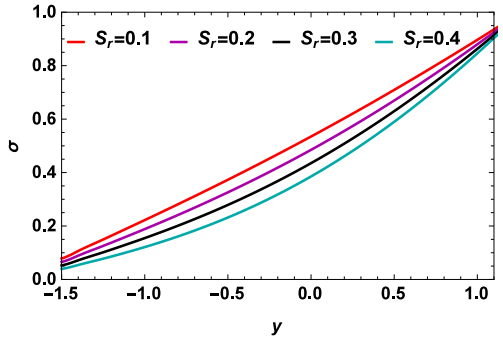

5f

Fig. 5: Variations in Concentration (ϕ) when $a = 0.4, b = 0.5, t = 0.2, x = 0.5, \phi = \frac{2\pi}{3}$

.

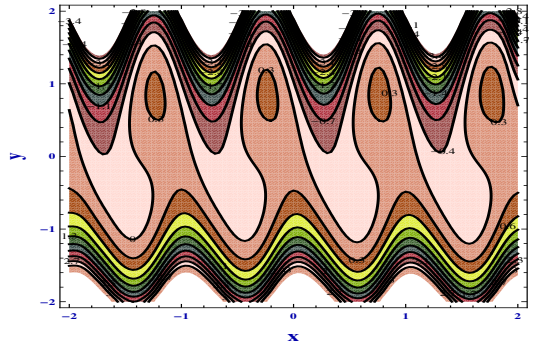

6c

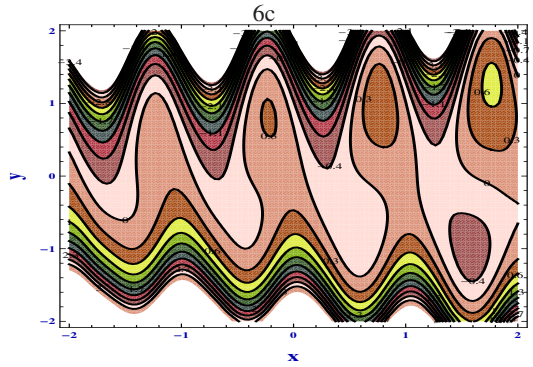

6d

Fig. 6: Effect of M in (a and b), m_1 in (c and d) on the Stream function ψ with $a = 0.3, b = 0.5, t = 0.5, \frac{dp}{dx} = -3, \phi = \frac{\pi}{3}, \Theta = \frac{\pi}{3}, \beta = 0.1$

.

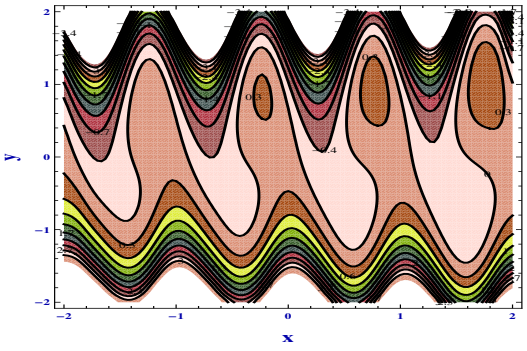

6a

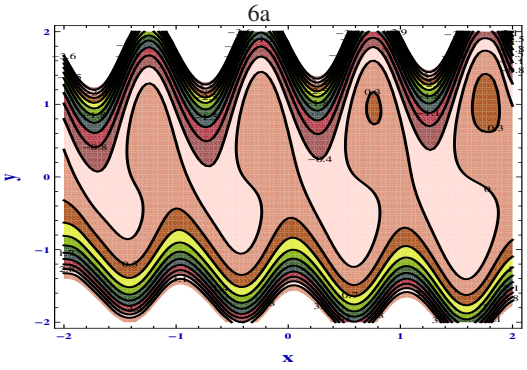

6b

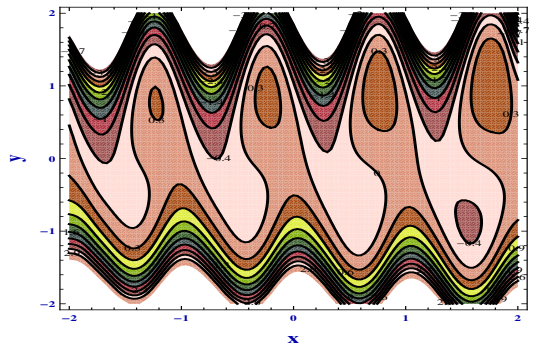

7a

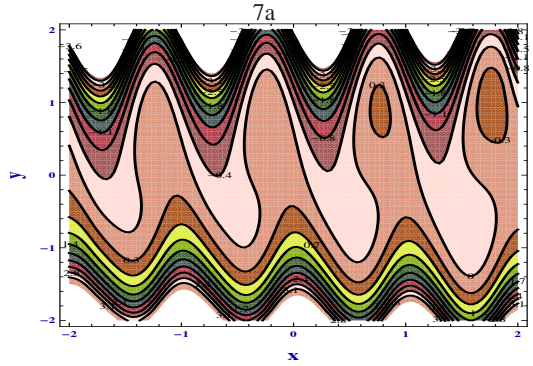

7b

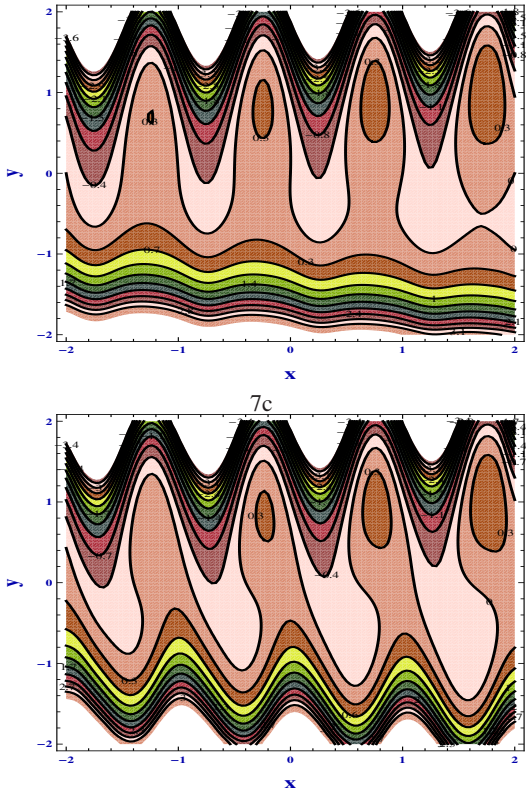

Fig. 7: Effect of N in (a and b), amplitude ratio (a) in (c and d), on the Stream function ψ with $a=0.3, b=0.5, t=0.5, \frac{dp}{dx}=-3, \phi=\frac{\pi}{3}, \Theta=\frac{\pi}{3}, \beta=0.1$

.

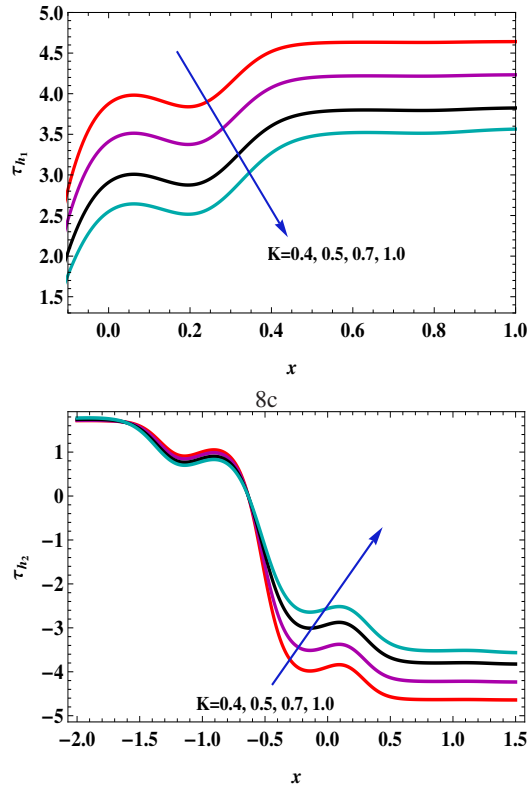

Fig. 8: Effect of M and K on the Skin Friction τ at h_1 and h_2 with $a=0.1, b=0.5, t=0.5, \frac{dp}{dx}=-2, \phi=\frac{\pi}{3}, \Theta=\frac{\pi}{3}, \beta=0.3$

.

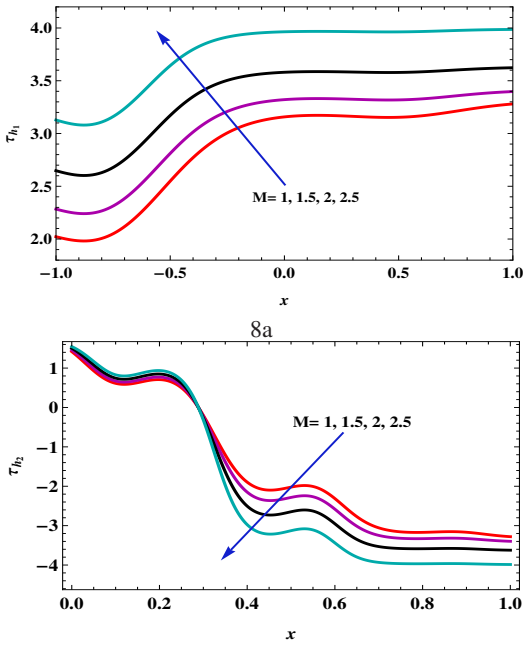

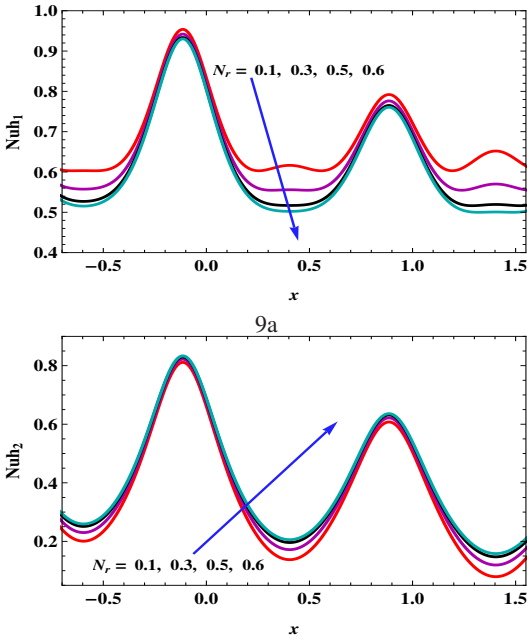

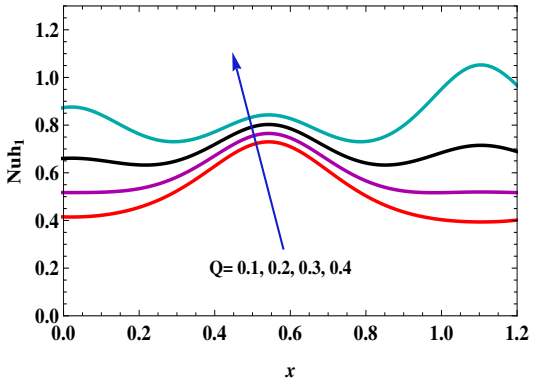

9c

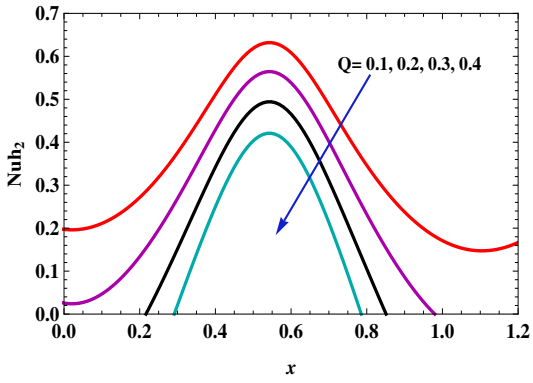

9d

Fig. 9: Effect of N_r and Q on the Nusselt Number N_u at h_1 and h_2 with $a = 0.4, b = 0.5, t = 0.2, \phi = \frac{\pi}{4}, P_r = 2, m_1 = 0.15$

.

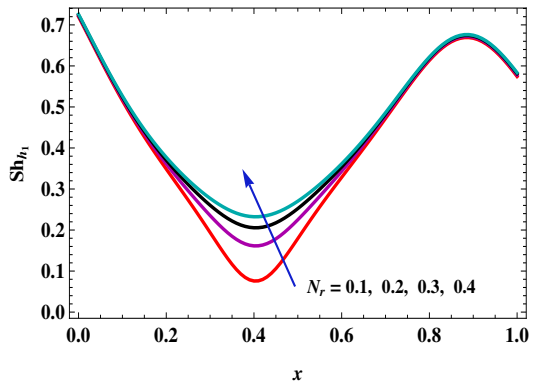

10a

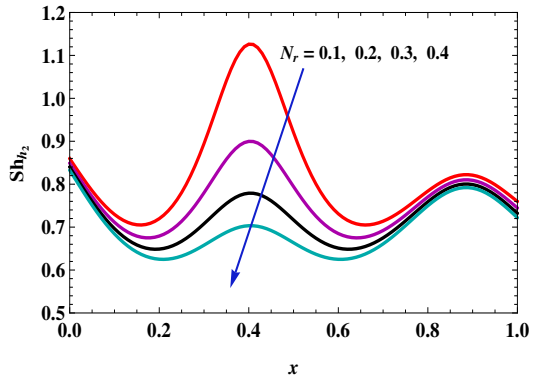

10b

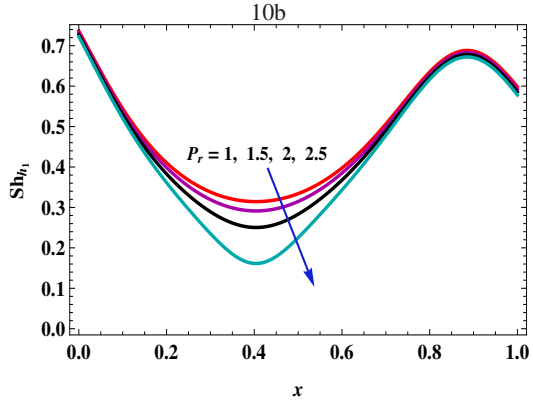

10c

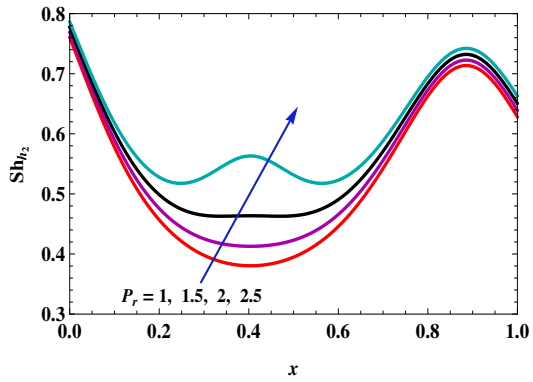

10d

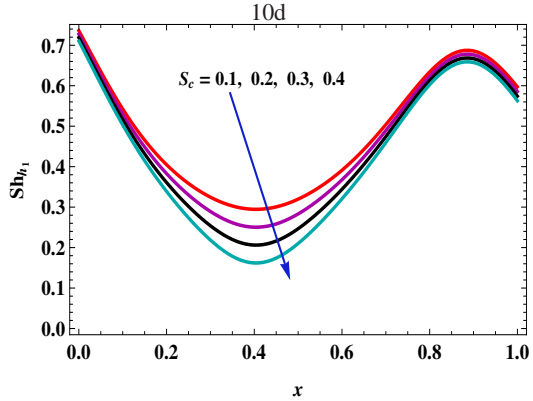

10e

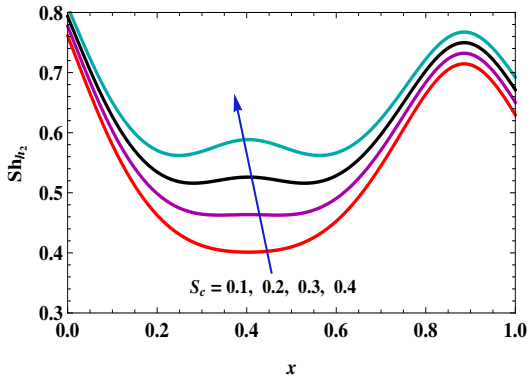

10f

Fig. 10: Effect of N_r, P_r and S_c on the Sherwood Number S_h at h_1 and h_2 with $a = 0.4, b = 0.5, t = 0.2, \phi = \frac{\pi}{4}, P_r = 2, m_1 = 0.15, Q = 0.5, S_r = 0.5$

.

–Increasing Prandtl number and heat source shows depression in concentration while thermal radiation accelerates the concentration.
–By increasing Soret and Schmidt numbers, the degree of concentration diminishes.
–The trapped bolus occurring near upper wall increases by increasing non-uniform parameter (m_1) but it decreases by increasing M and N and amplitude ratio (a).
–Skin friction increases by increasing magnetic field at h_1 while it decreases at h_2.
–Sherwood number increases at the top and decreases at the bottom of the channel by increasing Prandlt number.
–By increasing thermal radiation parameter, Nusselt number increases at the top of the channel while it decreases at the bottom of the channel.

References

[1] T.W. Latham, Fluid Motion in a Peristaltic Pump, MIT, Cambridge, MA, (1966).
[2] A.H. Shapiro, M.Y. Jaffrin, S.L. Weinberg, Peristaltic pumping with long wavelengths at low Reynolds number, Journal of Fluid Mechanics. 37, 799-825, (1969).
[3] O. Eytan , A.J. Jaffa , D. Elad, Peristaltic flow in a tapered channel: Application to embryo transport within the uterine cavity, Medical Engineering and Physics. 23, 473-482, (2001).
[4] M. Elshahed, M.H. Haroun, Peristaltic transport of Johnson?Segalman fluid under effect of a magnetic field, Mathematical Problems in Engineering. 2005, 663-667, (2005).
[5] T. Hayat, Y. Wang, A.M. Siddiqui, K. Hutter, S. Asghar, Peristaltic transport of a third order fluid in a circular cylindrical tube, Mathematical Models and Methods in Applied Sciences. 12, 1691-1706, (2002).
[6] Kh.S. Mekheimer, Peristaltic transport of blood under effect of a magnetic field in a non-uniform channels, Applied Mathematics and Computation. 153, 763-777, (2004).
[7] E.F. El Shehawey, Kh.S. Mekheimer, Couple-stresses in peristaltic transport of fluids, Journal of Physics D: Applied Physics. 27, 1163-1170, (1994).
[8] Y. Wang, T. Hayat, K. Hutter, Peristaltic flow of a Johnson?Segalman fluid through a deformable tube, Theoritical and Computational Fluid Dynamics. 21, 369-380, (2007).
[9] Kh. S. Mekheimer, Nonlinear peristaltic transport through a porous medium in an inclined planar channel, Journal of Porous Media. 6, 189-201, (2003).
[10] M. Kotkandapani, S. Srinivas, Nonlinear peristaltic transport of a Newtonian fluid in an inclined asymmetric channel through a porous medium, Physics Letters A. 372, 1265-1276, (2008).
[11] A.C. Eringen, Theory of micropolar fluids, Journal of Mathematics and Mechanics. 16, 1-16, (1966).
[12] G. Lukaszewicz, Micropolar Fluids-Theory and Applications, Birkhauser, (1999).
[13] O.Anwar Beg, R. Bhargava, and M. Rashidi, Numerical Simulation in Micropolar Fluid Dynamics. Lambert, Saarbrucken, Germany, (2011).
[14] E.A. Ashmawy, Fully developed natural convective micropolar fluid flow in a vertical channel with slip, Journal of the Egyptian Mathematical Society. 23, 563-567, (2015).
[15] Ajaz Ahmad Dar, K. Elangovan, Effect of Magnetic field and rotation on the micropolar fluid model of blood flow through stenotic arteries, International Journal of Biomedical Engineering and Technology. 26(2), 171-185, (2018).
[16] M. Muthtamilselvan, K. Periyadurai, Deog Hee Doh, Effect of uniform and nonuniform heat source on natural convection flow of micropolar fluid, International Journal of Heat and Mass Transfer. 115, 19-34, (2017).
[17] M. Kothandapani, V. Pushparaj, J. Prakash. Effect of magnetic field on peristaltic flow of a fourth grade fluid in a tapered asymmetric channel, Journal of King Saud University-Engineering Sciences. 30, 86-95, (2018).
[18] M. Ramzan, M. Farooq, T. Hayat, Jae Dong Chung, Radiative and Joule heating effects in the MHD flow of a micropolar fluid with partial slip and convective boundary condition, Journal of Molecular Liquids. 221, 394-400, (2016).
[19] B.I. Olajuwon, J.I. Oahimire, M. Ferdow, Effect of thermal radiation and Hall current on heat and mass transfer of unsteady MHD flow of a viscoelastic micropolar fluid through a porous medium, Engineering Science and Technology, an International Journal. 17, 185-193, (2014).
[20] Ajaz Ahmad Dar, K. Elangovan, Thermal diffusion, radiation and inclined magnetic field effects on oscillatory flow in an asymmetric channel in presence of heat source and chemical reaction, Journal of Nigerian Mathematical Society. 35, 488-509, (2016).
[21] S. Siddiqa, A. Faryad, N. Begum, M.A. Hossain, R. Subba Reddy Gorla, Periodic magnetohydrodynamic natural convection flow of a micropolar fluid with radiation, International Journal of Thermal Sciences. 111, 215-222, (2017).

[22] D Pal, S. Biswas, Magnetohydrodynamic convective-radiative oscillatory flow of a chemically reactive micropolasr fluid in a porous medium, Propulsion and Power Research. 7(2), 158-170,(2018).
[23] O. Eytan, D. Elad, Analysis of Intra-uterine fluid motion induced by uterine contractions, Bulletin of Mathematical Biology. 61, 221-238, (1999).
[24] O. Eytan, A.J. Jaffa, J. Har-Toov, E. Dalach, D. Elad, Dynamics of the intrauterine fluid-wall interface, Annals of Biomedical Engineering. 27, 372-379, (1999).
[25] M. Kothandapani and J. Prakash, Effect of radiation and magnetic field on peristaltic transport of nanofluids through a porous space in a tapered asymmetric channel, Journal of Magnetism and Magnetic Materials. 378, 152-163, (2015).
[26] R. Ellahi, S.U. Rahman, S. Nadeem, Noreen Sher Akbar, Influence of heat and mass transfer on micropolar fluid of blood flow through a tapered stenosed arteries with permeable walls, Journal of Computation and Theoritical Nanoscience. 11, 1156-1163, (2014).
[27] G.C. Shit, M. Roy, Effect of Slip Velocity on Peristaltic Transport of a Magneto-Micropolar Fluid Through a Porous Non-uniform Channel, International Journal of Applied and Computational Mathematics. 1, 121-141, (2015).
[28] B.C. Sarkar, S. Das, R.N. Jana and O.D.Makinde, Magnetohydrodynamic peristaltic flow of nanofluids in a convectively heated vertical asymmetric channel in presence of thermal radiation. Journal of Nanofluids, 4(4), 461-473, (2015).
[29] M.G. Reddy, B.C. Prasannakumara and O.D.Makinde, Cross diffusion impacts on hydromagnetic radiative peristaltic Carreau-Casson nanofluids flow in an irregular channel. Defect and Diffusion Forum, Vol. 377, pp 62-83, (2017).
[30] O. D. Makinde, M. Gnaneswara Reddy, K. Venugopal Reddy: Effects of Thermal Radiation on MHD Peristaltic Motion of Walters-B Fluid with Heat Source and Slip Conditions. Journal of Applied Fluid Mechanics, Vol. 10, No. 4, 1105-1112, (2017).
[31] K.V. Reddy, O.D. Makinde, M.G. Reddy: Thermal analysis of MHD electro-osmotic peristaltic pumping of Casson fluid through a rotating asymmetric microchannel. Indian Journal of Physics, Vol.92, Issue 11, 1439-1448, (2018).
[32] A.A. Dar, Effect of Thermal radiation, temperature jump and inclined magnetic field on the peristaltic transport of blood flow in an asymmetric channel with variable viscosity and heat absorption/generation. Iranian Journal of Science and Technology, Transactions of Mechanical Engineering, https://doi.org/10.1007/s40997-020-00349-6, (2020)

Ajaz Ahmad Dar received the PhD degree in Mathematics for Fluid Dynamics at Annamalai University, India. His research interests are in the areas of applied mathematics, mathematical biology, micropolar fluids and MHD Fluid Flows. He has published research articles in reputed international journals of mathematical and engineering sciences. He is referee and editor of mathematical journals.